24055

National Library of Canada | Bibliothèque nationale du Canada

CANADIAN THESES ON MICROFICHE | THÈSES CANADIENNES SUR MICROFICHE

NAME OF AUTHOR/NOM DE L'AUTEUR Harold Richard Hooper

TITLE OF THESIS/TITRE DE LA THÈSE The Use of Pulse Shapes to Measure Gamma Ray Polarization

UNIVERSITY/UNIVERSITÉ University of Alberta

DEGREE FOR WHICH THESIS WAS PRESENTED/ GRADE POUR LEQUEL CETTE THÈSE FUT PRÉSENTÉE Masters of Science

YEAR THIS DEGREE CONFERRED/ANNÉE D'OBTENTION DE CE GRADE 1975

NAME OF SUPERVISOR/NOM DU DIRECTEUR DE THÈSE D. M. Sheppard

Permission is hereby granted to the NATIONAL LIBRARY OF CANADA to microfilm this thesis and to lend or sell copies of the film.

The author reserves other publication rights, and neither the thesis nor extensive extracts from it may be printed or otherwise reproduced without the author's written permission.

L'autorisation est, par la présente, accordée à la BIBLIOTHÈQUE NATIONALE DU CANADA de microfilmer cette thèse et de prêter ou de vendre des exemplaires du film.

L'auteur se réserve les autres droits de publication; ni la thèse ni de longs extraits de celle-ci ne doivent être imprimés ou autrement reproduits sans l'autorisation écrite de l'auteur.

DATED/DATÉ April 1, 1975 SIGNED/SIGNÉ H. Richard Hooper

PERMANENT ADDRESS/RÉSIDENCE FIXE 2171 Bel-Air Dr, Ottawa, Ontario, K2C 0X2

NL-91 (3-74)

THE UNIVERSITY OF ALBERTA

THE USE OF PULSE SHAPES TO MEASURE GAMMA RAY POLARIZATION

by

© HAROLD RICHARD HOOPER

A THESIS

SUBMITTED TO THE FACULTY OF GRADUATE STUDIES AND RESEARCH

IN PARTIAL FULFILLMENT OF THE REQUIREMENTS FOR THE DEGREE

OF MASTER OF SCIENCE

DEPARTMENT OF PHYSICS

EDMONTON, ALBERTA

SPRING, 1975

THE UNIVERSITY OF ALBERTA

FACULTY OF GRADUATE STUDIES AND RESEARCH

The undersigned certify that they have read, and recommend to the Faculty of Graduate Studies and Research, for acceptance, a thesis entitled THE USE OF PULSE SHAPES TO MEASURE GAMMA RAY POLARIZATION submitted by Harold Richard Hooper in partial fulfillment of the requirements for the degree of Master of Science.

Douglas M. Sheppard
Supervisor

Jack W. Macki

Peter J. Kuper

A. J. MacDonald

Date: March 14, 1975

Abstract

An investigation is made as to whether or not pulse shapes within a single planar Ge(Li) detector can be used to measure gamma ray polarization. Compton scattering polarization effects are studied experimentally and theoretically using both a Triple Constant Fraction Pulse Shape Discriminator and a differentiating pulse shape analyser. As well, a short theoretical study is made of photoelectric absorption polarization effects. The results of these studies show that pulse shape analysis in a Ge(Li) detector is not a practical method of measuring gamma ray polarization.

Acknowledgements

I would like to express my gratitude to Dr. D.M. Sheppard and Dr. W.J. McDonald for their support and guidance during the course of this work.

As well I wish to thank Dr. G.C. Neilson for initially proposing the idea, and for providing various helpful suggestions when they were needed.

I am especially indepted to Dr. David Hutcheon for his helpful insight into the physical and computational aspects of the problem.

Finally, a special thanks is due to Jim Easton for his help in much of the computer work.

QUEEN'S
BELFAST

TABLE OF CONTENTS

Chapter		Page
1.	INTRODUCTION	1
2.	THEORY	3
	2.1 Compton Scattering and Polarization Measurement	3
	2.2 Pulse Shapes in a p-i-n Detector	6
3.	MEASUREMENT OF PULSE SHAPES	13
	3.1 The Triple Constant Fraction Pulse Shape Discriminator	13
	3.2 A Possible New Method of Shape Measurement	22
4.	CONCLUSIONS	29
REFERENCES		32
APPENDIX 1.	POLARIZATION EFFECTS IN PHOTOELECTRIC ABSORPTION	33
APPENDIX 2.	MONTE-CARLO COMPTON SCATTERING SIMULATION PROGRAM	41

LIST OF TABLES

Table		Page
1	Polarization sensitivity in a planar Ge(Li) detector at a gamma ray energy of 0.847 MeV.	25
2	Polarization sensitivity as a function of gamma ray energy in a planar detector of thickness 3.4 cm.	25
3	Polarization sensitivity of various Ge(Li) polarimeters at a gamma energy of 0.847 MeV.	30

LIST OF FIGURES

Figure		Page
1	Compton Scattering Terminology	4
2	Experimental Asymmetry in Gamma Ray Polarimeters	7
3	Formation of Pulse Shapes in a Planar Ge(Li) Detector	9
4	Electron Range as a Function of Energy	11
5	Photographs of pulse shapes obtained using a planar Ge(Li) detector and a ^{60}Co gamma ray source.	12
6	Triggering in a CFT	14
7	Delta as a function of gamma interaction type and location (a = 0.5 arbitrary units).	16
8	Delta as a function of gamma interaction type and location (a > 2.0 arbitrary units).	17
9	Experimental Delta Spectra for a Thin Planar Detector	19
10	Delta Spectra for a Thick Planar Detector	21
11	Derivative of a one-compton pulse shape.	23
12	Pulse shape derivative assuming a sharp pulse shape.	23
13	Identical Pulse Shape Derivatives	27
14	Energy dependence in the photoelectric effect of θ_{max} and $A(\theta_{max})$	35
15	Average spreading of electrons as a function of distance travelled in a Ge(Li) detector.	38
16	Electron energy as a function of total distance travelled in a Ge(Li) detector.	39

Chapter I

Introduction

During the past decade considerable progress has been made in the development of nuclear semiconductor detectors. The introduction of large volume lithium drifted germanium, or Ge(Li), detectors has provided experimenters with an instrument for gamma ray detection which combines both excellent energy resolution with reasonable overall detection efficiency. The use of this device has therefore led to advances in many areas of nuclear gamma ray studies, including that branch which deals with gamma polarization measurement. As a result, in recent years a number of gamma polarimeters, all capable of good energy resolution, have been developed.

These polarimeters, which make use of the scattering asymmetry inherent in the compton scattering process, have included both conventional two- and three-crystal compton polarimeters and single crystal planar detectors. The planar detectors, in particular, appear to be quite attractive, due to their simplicity of experimental setup. Not only are they simpler physically to arrange and manipulate, but also they are less complicated electronically to work with, since they do not require much of the excess electronic equipment necessary to handle a multidetector coincidence system. However, recent studies have shown that, although the planar detector has a higher overall detection efficiency than

multicrystal systems, its relative polarization sensitivity is quite small. Hence it would be of considerable benefit to design a single crystal gamma detector capable of high polarization sensitivity.

This thesis investigates the question of whether or not pulse shapes within a single detector can be used to measure the polarization asymmetry produced by compton scattering. Two different methods of measuring these shapes are explained, and their individual merits and deficiencies discussed. As well, a short appendix is included which studies the polarization effect inherent in the photoelectric absorption of gamma photons.

Chapter II

Theory

2.1 Compton Scattering and Polarization Measurement

It can be shown that the differential collision cross section for the scattering of incident plane-polarized radiation is given by

$$\frac{d\sigma}{d\Omega} = \frac{r_o^2}{4}\left(\frac{\nu'}{\nu_o}\right)^2\left(\frac{\nu_o}{\nu'} + \frac{\nu'}{\nu_o} - 2 + 4\cos^2\chi\right)$$

where χ is the angle between the electric vectors of the incident and scattered radiation, $h\nu_o$ is the energy of the incident photon, $h\nu'$ the energy of the scattered photon, and r_o the classical electron radius. The angles and directions encountered in the compton scattering process are visualized in fig. 1, in which:

OA = direction of scattered photon,

OAB = scattering plane,

Θ = scattering angle,

ε_o = electric vector of incident photon,

ξ = angle between ε_o and OA,

ODB = plane of polarization of incident radiation,

ϕ = angle between plane of incident polarization and scattering plane,

ε' = electric vector of scattered photon,

$\varepsilon'_{\parallel}$ = projection of ε' on OAC plane,

$\varepsilon'_{\perp}$ = projection of ε' perpendicular to OAC plane,

β = angle between ε' and OAC plane, and

χ = angle between ε' and ε_o.

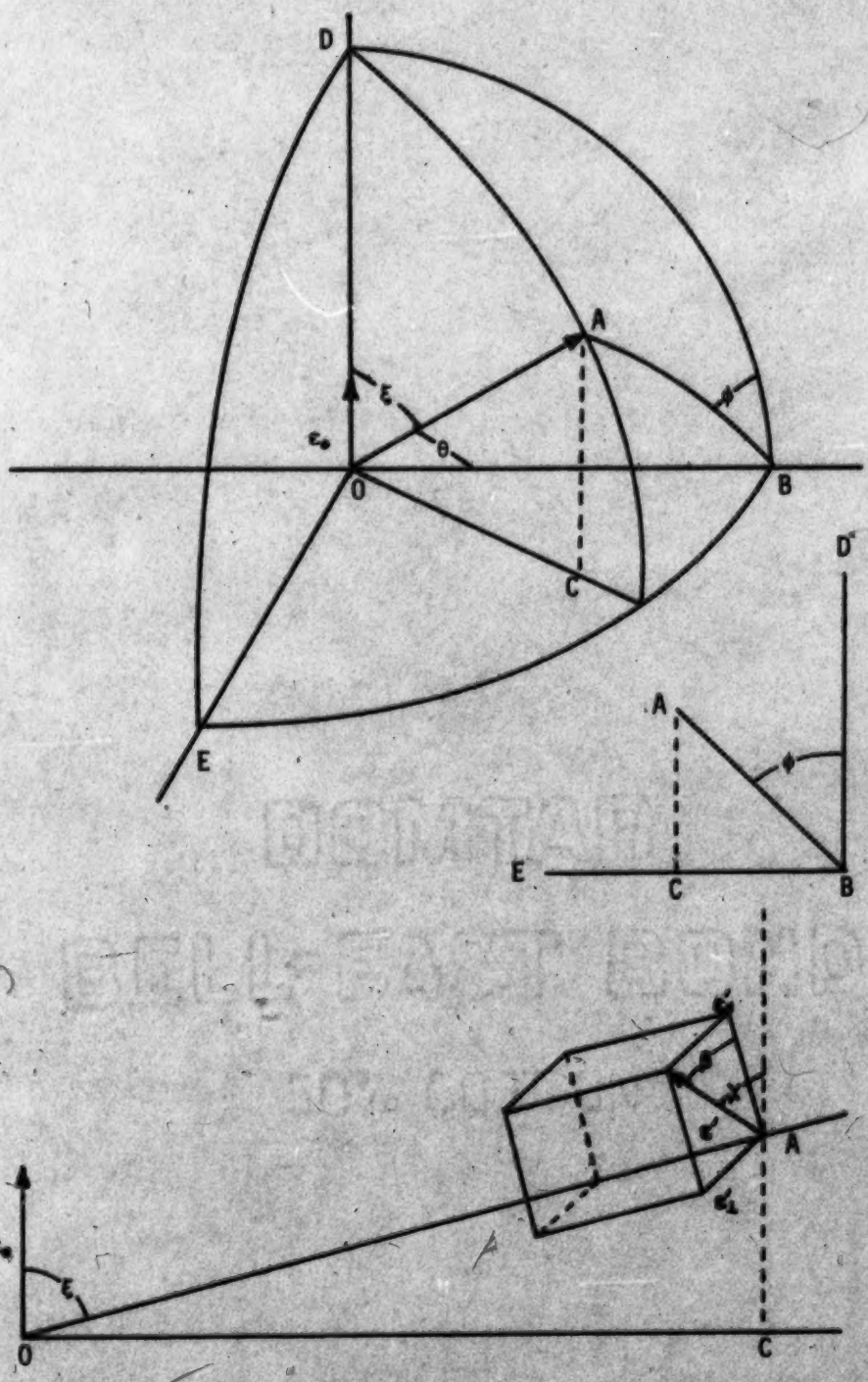

Figure 1 Compton Scattering Terminology

The energy of the scattered photon is given by:

$$h\nu' = \frac{m_0c^2}{1-\cos\theta + (1/\alpha)}$$

where

$$\alpha = \frac{h\nu_0}{m_0c^2} .$$

Thus

$$\frac{\nu'}{\nu_0} = \frac{1}{1+\alpha(1-\cos\theta)}$$

By geometrical arguments it can be shown that

$$\cos\chi = \cos\beta \sin\xi$$

and

$$\cos\xi = \sin\theta \cos\phi .$$

Therefore, summing over all possible directions of final polarization,

$$\frac{d\sigma}{d\Omega} = \frac{r_0^2}{2}\left(\frac{\nu'}{\nu_0}\right)^2\left(\frac{\nu_0}{\nu'} + \frac{\nu'}{\nu_0} - 2\cos^2\xi\right)$$

$$= \frac{r_0^2}{2}\left(\frac{\nu'}{\nu_0}\right)^2\left(\frac{\nu_0}{\nu'} + \frac{\nu'}{\nu_0} - 2\sin^2\theta\cos^2\phi\right).$$

Hence it is apparent that plane-polarized radiation will tend to be scattered in a plane perpendicular to the plane of polarization of the incident radiation ($\phi = 90°$).

This polarization effect is used as the basis for many polarization measuring devices, including the two- and three-crystal compton polarimeters and the single crystal planar detector. The standard experimental procedure involves the measurement of a scattering asymmetry A, defined by $A = QP$, where P is the linear polarization of the incident photon beam ($-1 \leq P \leq +1$),

and Q is the polarization sensitivity of the detector ($0 \leq Q \leq +1$). "A" is measured by comparing the counting rates of the polarimeter when oriented in the $\omega = 0^\circ$ direction and the $\omega = 90^\circ$ direction (see fig. 2).

Thus $$A = \frac{N(90^\circ) - N(0^\circ)}{N(90^\circ) + N(0^\circ)}$$

where $N(\omega)$ = the number of counts occuring in the detector when it is oriented at the angle ω.

There are two ways this asymmetry in scattering can be detected when only using a single detector. To begin with, the detector crystal can be of some shape which preferentially absorbes photons scattered in a particular direction, as is the case for a planar detector. Unfortunately, the polarization sensitivity of this experimental setup is quite poor, even though its overall detection efficiency is high. Hence it is normally used only in cases where the overall accuracy of a polarization measurement is limited by its counting statistics.

Secondly, though, the scattering asymmetry could be measured within a single crystal by considering the shape of the electronic pulses triggered within it. To understand how this could be done, one must first understand how electronic signals are formed in Ge(Li) detectors, and as well how they can or could be measured.

2.2 Pulse Shapes in a p-i-n Detector

The simplest way to determine the pulse shape produced by a planar Ge(Li) detector is to first consider

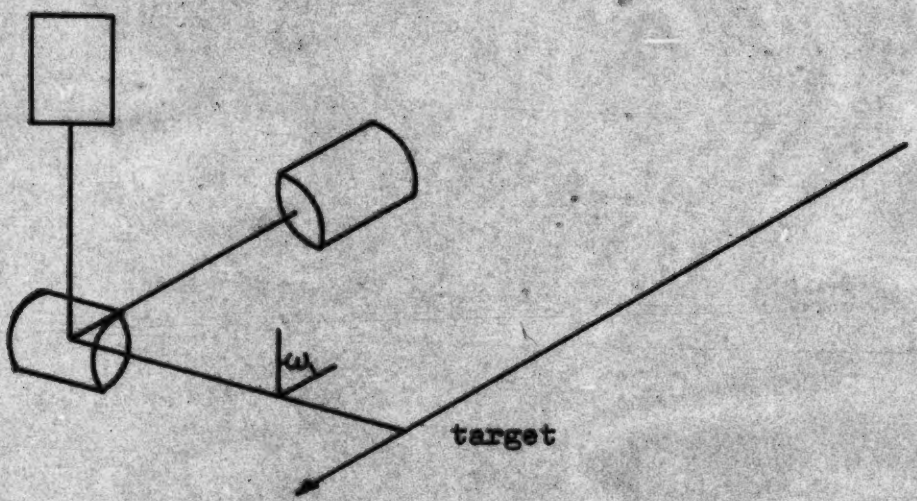

Three-Crystal Compton Polarimeter

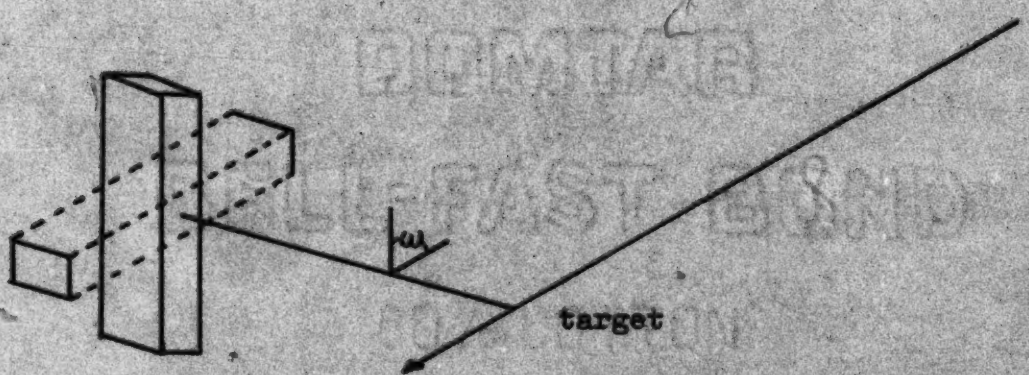

Thin Planar Detector

Figure 2 Experimental Asymmetry in Gamma Ray Polarimeters

the shape produced when only a single electron-hole (e-h) pair is created within the detector crystal. This situation is depicted in fig. 3a, in which d is the detector thickness, V the voltage drop across it, and Z_o the distance from the creation point of the e-h pair to the crystal's p layer. If μ_e and μ_h are the electron and hole mobilities, then the currents in the external circuit due to the electron and hole are

$$i_e = (V/d^2)\, q\, \mu_e$$

and $$i_h = (V/d^2)\, q\, \mu_h$$

where of course q is just the elementary charge of an electron. The time taken for the electron and hole to reach the outer layers of the detector is

$$T_e = \{(d - Z_o)/\mu_e\}\, (d/V)$$

and $$T_h = \{Z_o/\mu_h\}\, (d/V)\ .$$

Since the final output signal is just the sum of the integrated electron and hole current signals, the total signal out of the detector is as shown in fig. 3b. Note that the total charge flow in the external circuit is

$$Q_{total} = i_e T_e + i_h T_h$$
$$= q\ .$$

Most germanium detectors, and in particular Ge(Li) detectors are operated at a temperature of about 77°K. At this temperature the electron mobility in germanium is approximately equal to the hole mobility, and thus $i_e = i_h$. Assuming, therefore, that the electric field inside the planar Ge(Li) is in fact a constant throughout

Figure 3 Formation of Pulse Shapes in a Planar Ge(Li) Detector

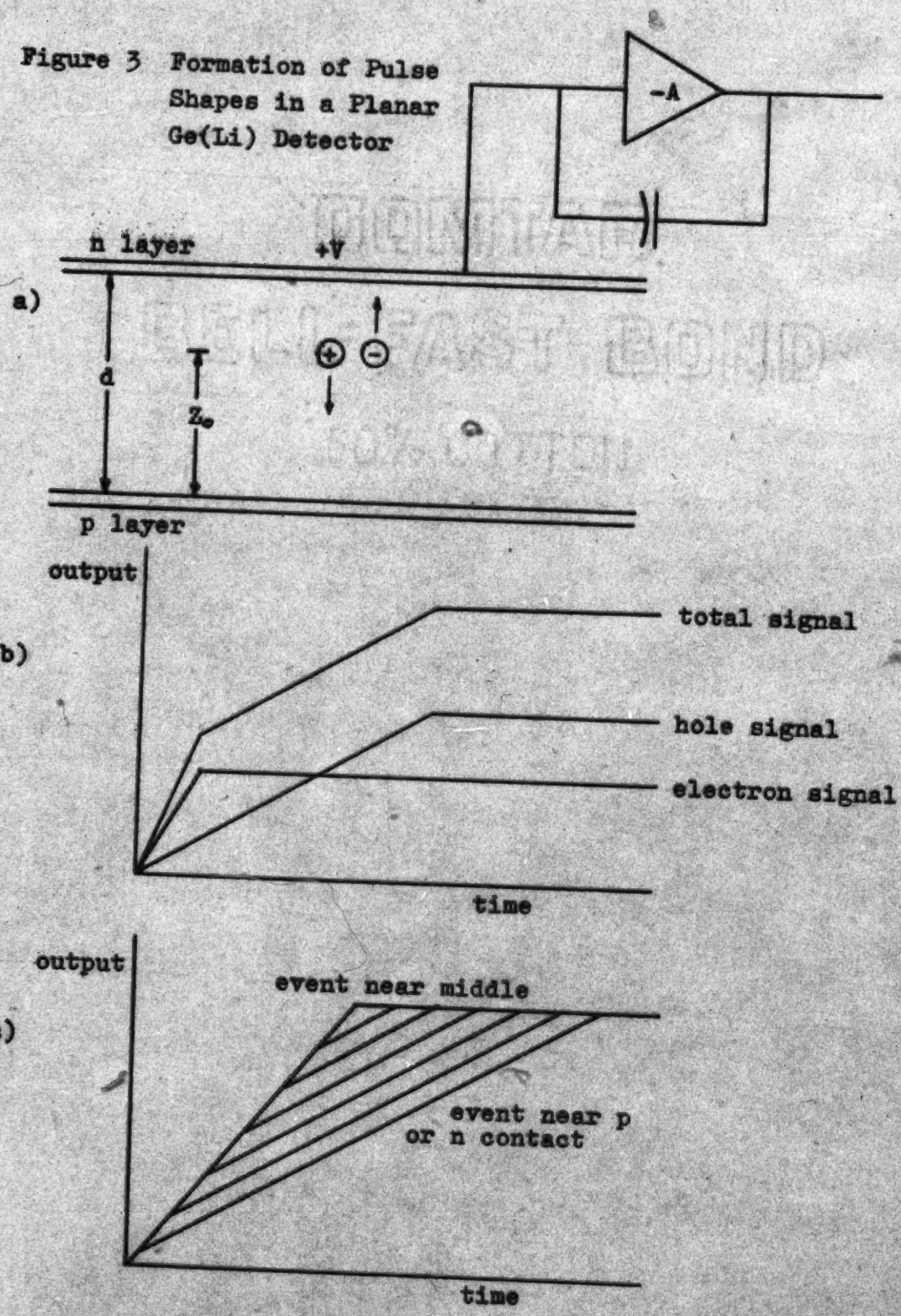

the crystal, and that electronic noise in the system is minimal, the total output signal for a single e-h pair will appear as in fig. 3c. It should be noted here that the shape of the signal is dependent upon the location of creation of the e-h pair.

Of course all of the above discussion is quite simplified when compared to what actually happens in the lab. During a gamma-ray detection experiment a single photon may be photo-absorbed, compton scattered, or absorbed by pair-production within the Ge(Li) crystal. At each point in the detector where the gamma loses some energy, a large number of e-h pairs are produced. Furthermore, the "point" at which they are produced has finite dimensions, which depend both on the gamma energy lost there (see fig. 4) and the scattering kinematics of the ionized electrons. Thus the real pulse shapes produced by a planar Ge(Li) detector are similar to those shown in fig. 5.

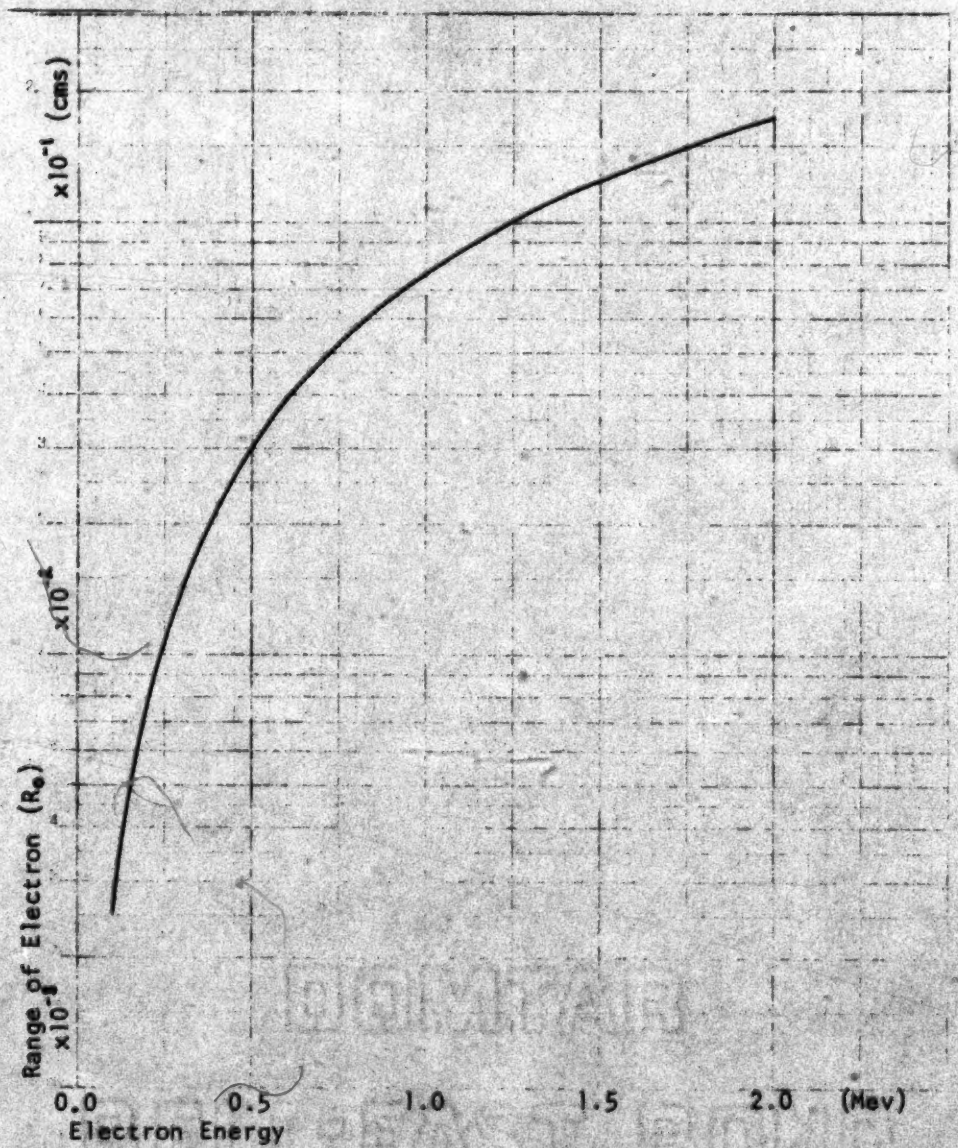

Figure 4 Electron Range as a Function of Energy

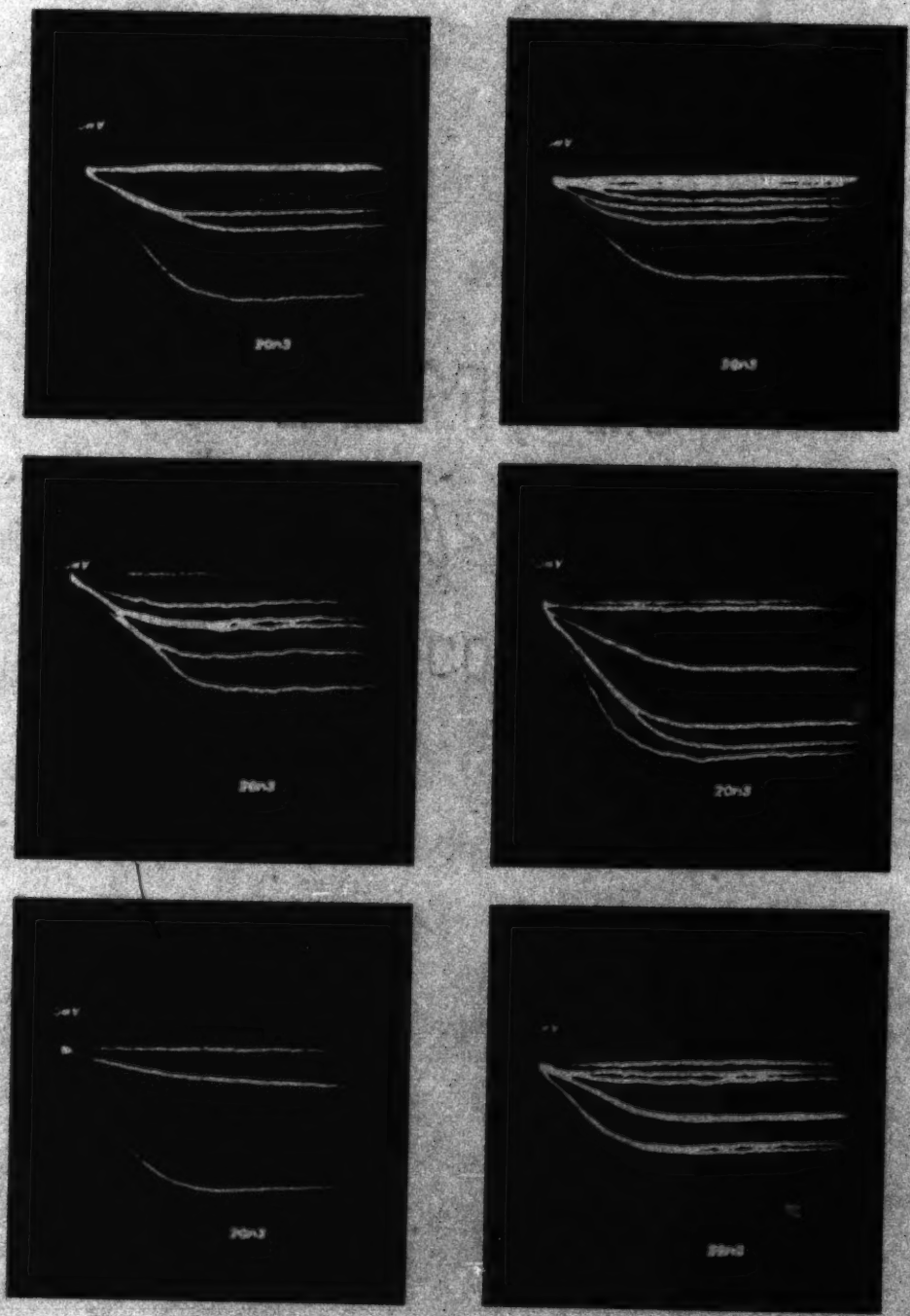

Figure 5 Photographs of pulse shapes obtained using a planar Ge(Li) detector and a ^{60}Co gamma ray source. The particular preamplifier used with this detector provided a negative output signal.

Chapter III

Measurement of Pulse Shapes

3.1 The Triple Constant Fraction Pulse Shape Discriminator

Theory:

Once the general appearance of the pulse shapes is known, the question arises as to whether or not these pulse shapes can be "measured", and if indeed these measurements are sensitive to the polarization effect discussed earlier. One device which has been used in the past to measure pulse shape is the triple constant fraction pulse shape discriminator (TCF).)[1]

The TCF makes use of two constant fraction timing triggers (CFT) to measure pulse shape. Each CFT sees an input pulse with a leading edge of some shape g(t), and inverts and shrinks it in amplitude by a fraction f_1 (see fig. 6). The CFT then combines this smaller pulse with the original pulse, which has been delayed by a time interval "a", and triggers when the resultant pulse crosses zero. This occures at a time t_1, such that

$$g(t_1) = f_1 g(t_1 + a) .$$

Note that for a linear pulse

$$g(t) = mt$$

$$\therefore t_1 = \frac{f_1 a}{1 - f_1} .$$

Thus t_1 is independent of the slope m. In a TCF one CFT is set at a fraction f_1 and used to trigger a start signal in a time-to-analog converter (TAC), while another

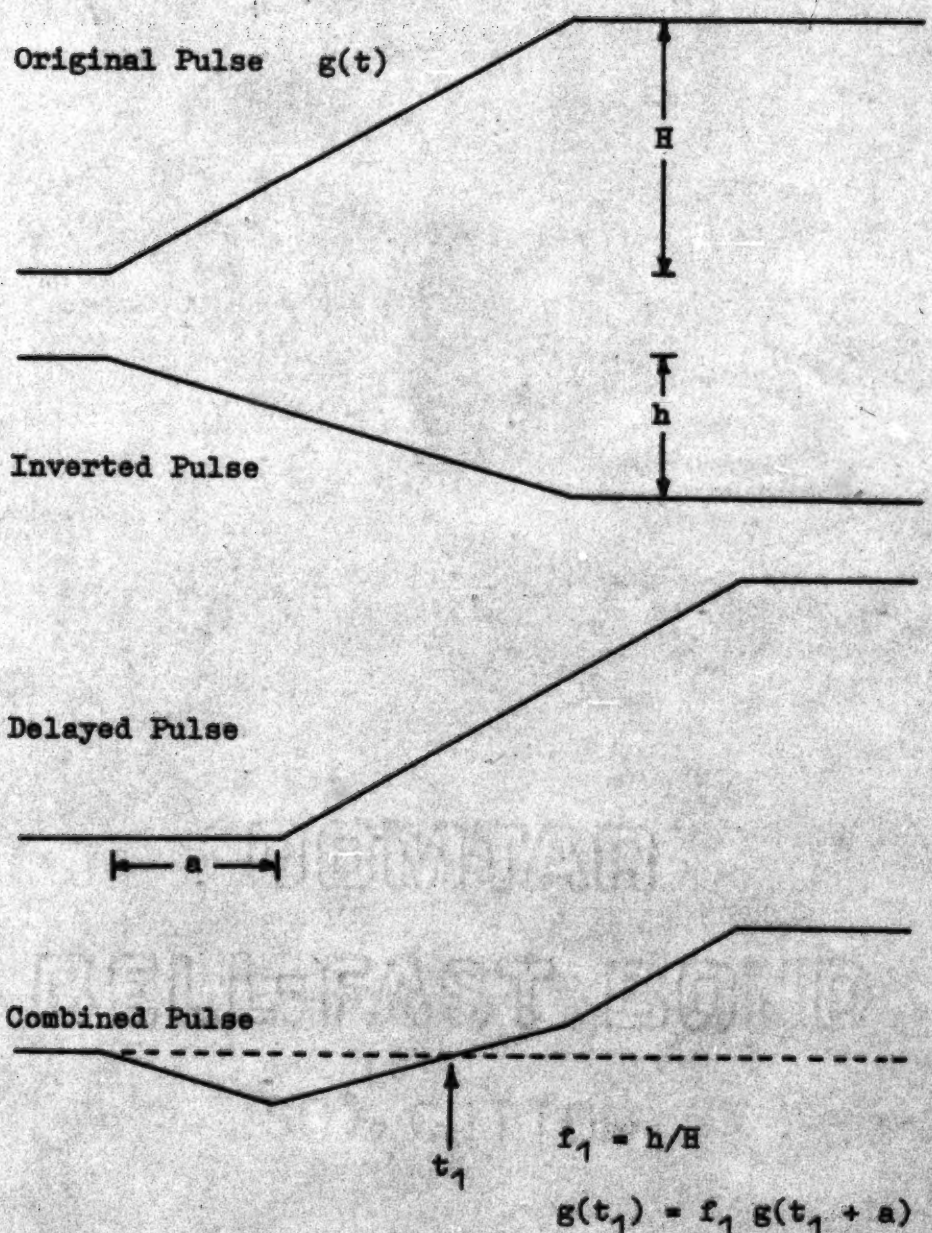

Figure 6 Triggering In A CFT

CFT is set to a larger fraction f_2 and used to trigger a stop pulse in the TAC. This then defines a time interval δ, such that $\delta = t_2 - t_1$ where

$$g(t_1) = f_1 g(t_1 + a)$$

and $$g(t_2) = f_2 g(t_2 + a).$$

δ can therefore be used as a rough measurement of the pulse shapes. For instance, note that for a pulse with a linear leading edge:

$$\delta = a \frac{f_2 - f_1}{(1-f_2)(1-f_1)}$$

$$= \text{constant.}$$

Of course the interpretation of δ becomes much more difficult when real pulse shapes of the kind shown in fig. 5 are encountered. δ is highly dependent upon the type and energy of the interaction encountered, the position or positions of the interaction, and in particular the delay setting "a" of the TCF. Figs. 7 and 8 show the various δ which would be expected for photoelectric and one-compton events occuring at various locations throughout the crystal. In these graphs:

a = the delay setting on the TCF,

Z_1 = the location of the outermost gamma interaction, (0 refers to the center of the crystal, 1 to the detector edge),

Z_2 = the location of the innermost gamma interaction, and

W_i = the amount of the total gamma energy deposited at location Z_i.

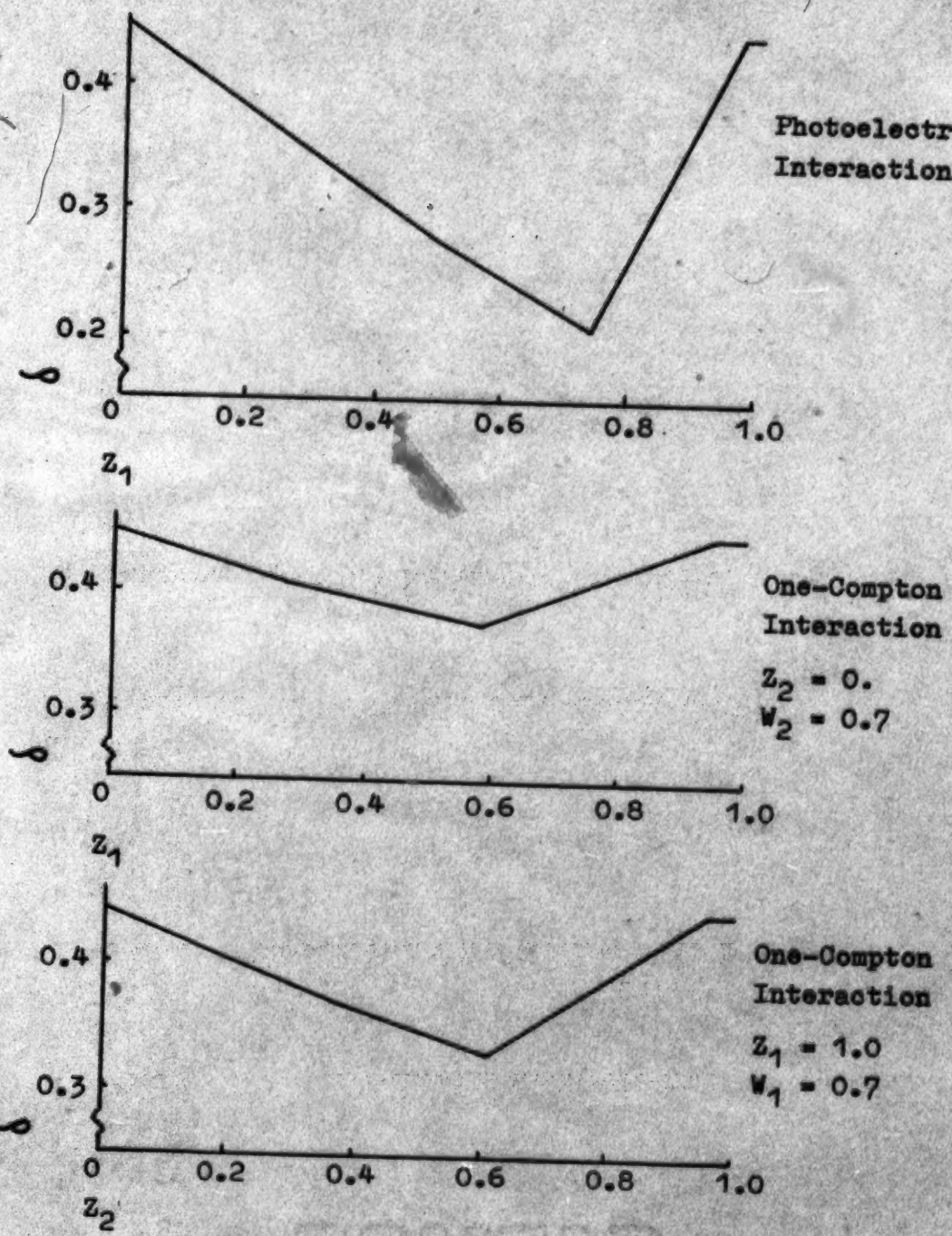

Figure 7 Delta as a function of gamma interaction type and location (a = 0.5 arbitrary units). Delta is measured in arbitrary units.

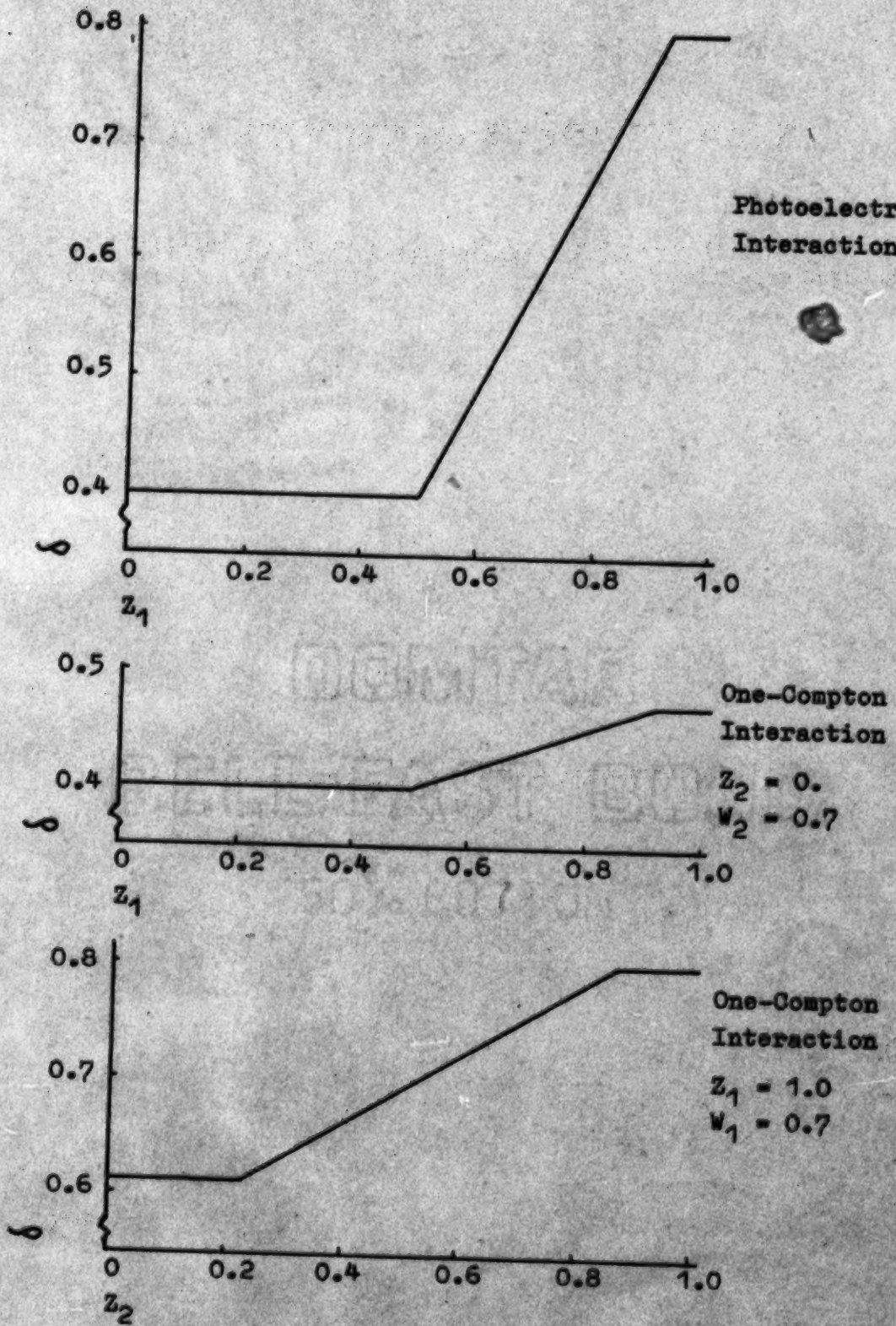

Figure 8 Delta as a function of gamma interaction type and location ($a > 2.0$ arbitrary units).

For the purpose of these graphs, all pulse shapes were considered to be sharp; that is the range R_e of all scattered electrons was assumed to be zero.

Results:

The shape of a δ spectrum and its sensitivity to polarization were first investigated experimentally using a thin planar detector. This detector had a radius of 1.73 cm and a thickness of 0.6 cm. In the experiment 3.4 MeV protons were used to excite ^{56}Fe nuclei to their first excited state, from which they decayed emitting photons of energy 0.847 MeV. Angular correlation measurements showed that this radiation had a polarization at 90° of (0.51±0.03), while at 0° its polarization was zero. Shape spectra were accumulated and compared at these two angles to see if any differences could be distinguished. However, for a constant delay setting, the two shape spectra were found to be identical (see fig. 9).

This result is actually not too surprising. It can be shown that the pulse shapes formed in a <u>thin</u> detector tend to be smeared out because of the finite electron scattering radius, and hence any subtle shape differences which would occur due to a polarization effect could be destroyed. An example of this effect will be discussed later. What is required for good shape measurements is a reasonably thick planar detector, in which the average

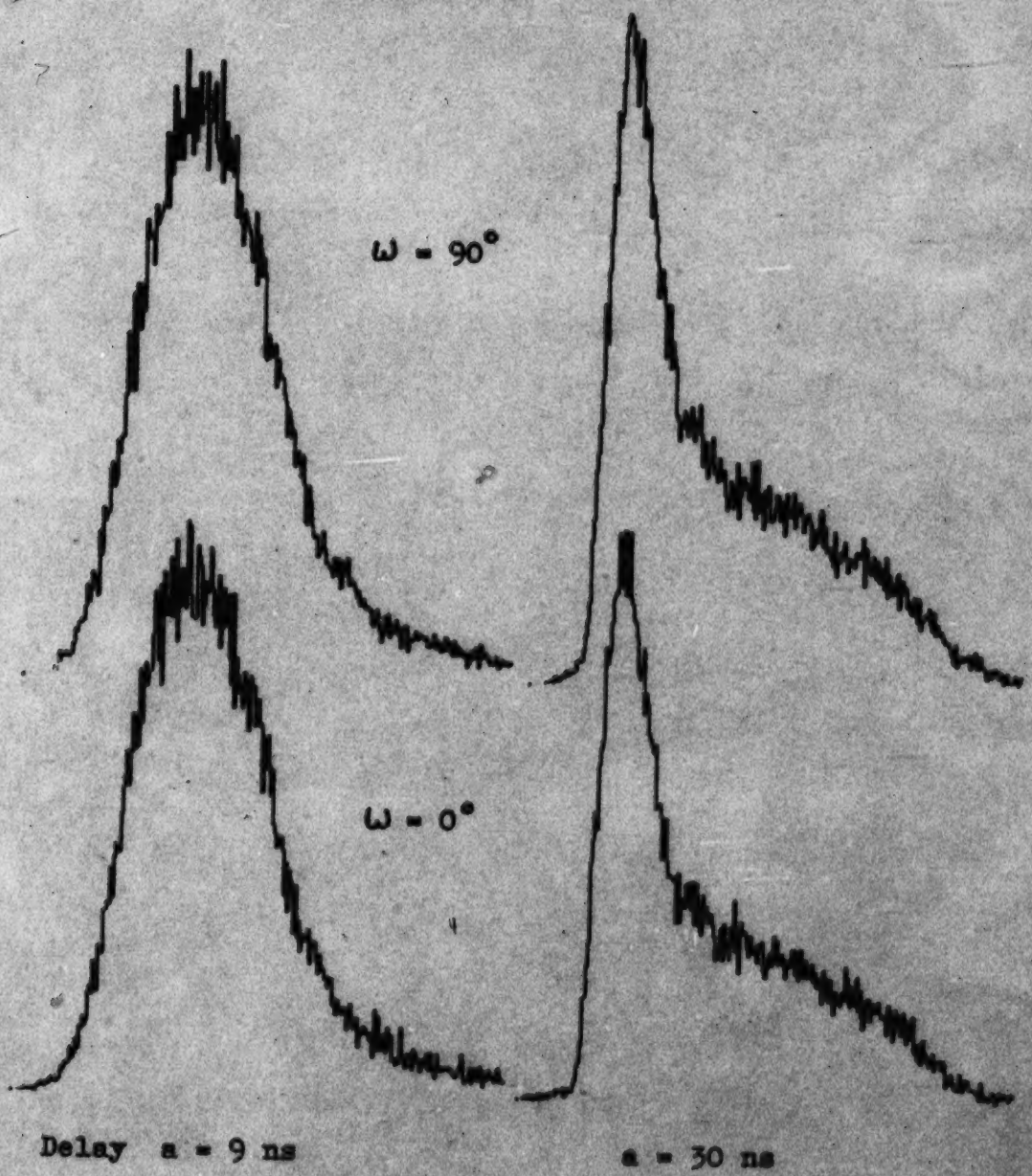

Figure 9 Experimental Delta Spectra For A Thin Planar Detector

photon scattering distance is much larger than the electron scattering radius R_e. However, since no such detector was available for experimentation in the lab, further experimental results had to be simulated using Monte-Carlo computing techniques.

The results of these computer programs are shown in fig. 10. These graphs illustrate the one-compton δ spectrum for a detector of radius 1.73 cm and thickness 3.4 cm, oriented at $\omega = 0^\circ$ and 90°. A 0.4 MeV gamma source with a polarization of +1 was assumed, and all pulse shapes were considered to be sharp. The statistical error in these graphs is estimated to be $\pm 10\%$. It should be noted that the actual δ spectrum for this experiment would include other contributions from both photoelectric and multicompton events, and since these interactions are for the most part polarization insensitive, they will tend to decrease any polarization effect inherent in the one-compton δ spectrum.

These graphs suggest that δ is not very sensitive to the small polarization effect discussed above. This result was already hinted at in figs. 7 and 8, which demonstrated that δ as measured by a TCF is a very poor measure of the seperation of events occuring in a one-compton scattering interaction. Thus it is extremely doubtful that polarization could be measured using such a device.

Figure 10 Delta Spectra For A Thick Planar Detector

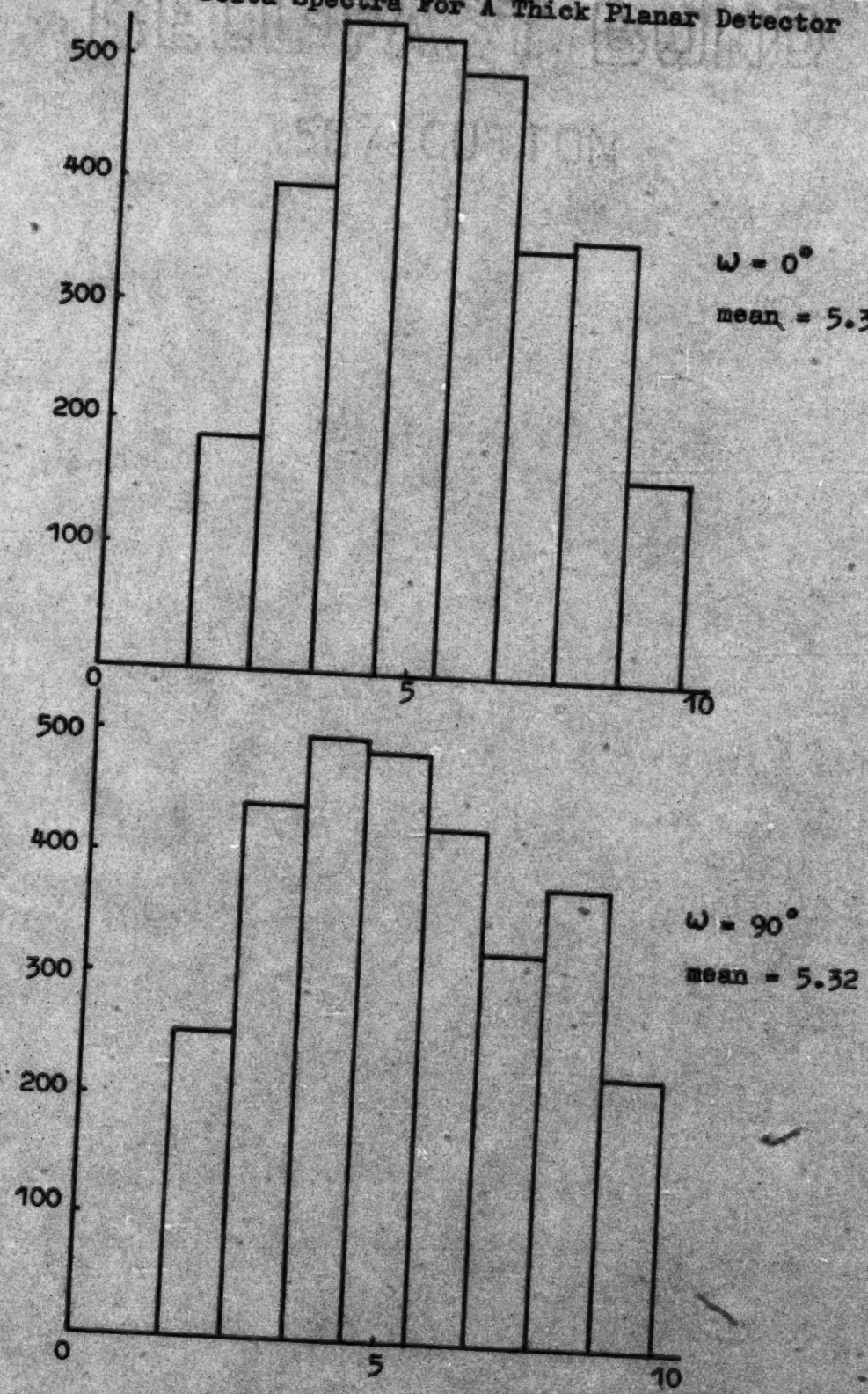

3.2 A Possible New Method of Shape Measurement

Theory:

One problem encountered by the TCF was that its output was partially dependant upon the location of the first gamma interaction in the detector. It would be of an obvious advantage to design a pulse shape measurement device whose output depended only upon the separation of the two gamma interactions in a one-compton scattering event, and not upon the individual location of either interaction.

Fig. 11 shows the derivative of the pulse shapes shown earlier. It will be noticed that the position of the first "kink" in this pulse shape occures at a time $t_1 \propto d/2 - Z_1$, where d/2 is the half thickness of the detector, and Z_1 the distance in the x direction from the nearest detector edge to the outermost gamma interaction. Similarly the second kink occures at a time $t_2 \propto d/2 - Z_2$, where Z_2 is the distance from the nearest detector edge to the other gamma interaction. Hence notice that

$$\xi \equiv t_2 - t_1$$
$$\propto Z_2 - Z_1 .$$

Thus an ξ spectrum of many one-compton pulse shapes should be polarization sensitive.

Recently a new pulse shape analyser has been developed which may be capable of making ξ measurements.)[2] However, several factors dictate what an overall ξ

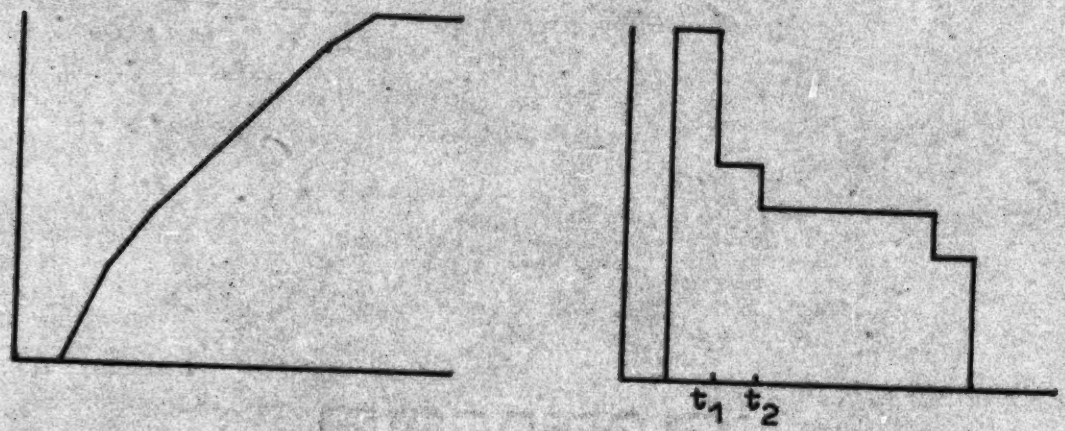

Figure 11 Derivative of a one-compton pulse shape.

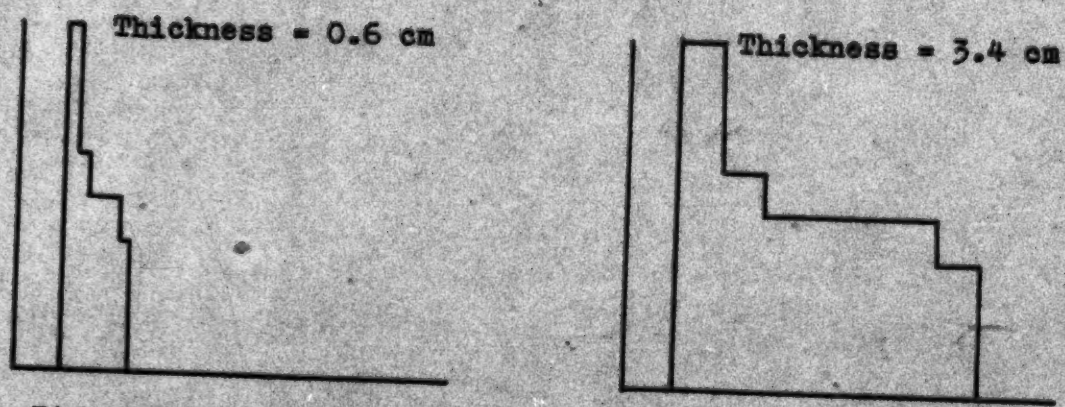

Figure 12 Pulse shape derivative assuming a sharp pulse shape.

spectrum will actually look like, and these should be considered before any experimental work is carried out. They are:

Detector Thickness It is obvious that as the thickness of a detector is decreased, so to will its maximum ξ value and average ξ value decrease. Therefore a thick detector will have a higher polarization sensitivity than a thin detector (see table 1).

Electron Range Fig. 4 showed the range R_o of an electron of energy E MeV inside a germanium crystal. This finite range will tend to smooth out the kinks in the various pulse shapes produced, and can as suggested earlier completely obliterate them. For example fig. 12 shows the expected pulse shape derivatives, without considering electron range, for typical one-compton gamma interactions in two planar detectors of different thickness. It is apparent that, if the electron range effect were taken into consideration, the pulse shape derivative for the thinner detector would be less distinct than that of the thicker detector. Hence the thinner crystal is again found to provide ξ measurements which are less polarization sensitive.

Photoelectric Effect Photoelectric events within a detector will provide ξ measurements which are polarization insensitive. Hence at low energies where the photoelectric effect dominates over compton effects, the detector will lose its polarization sensitivity.

Detector Thickness (cm)	One-Compton Events			All Events		
	ε_{mean} ω=0 (mm)	ε_{mean} ω=90 (mm)	Q	ε_{mean} ω=0 (mm)	ε_{mean} ω=90 (mm)	Q
0.6	0.86±0.04	0.68±0.03	0.12±0.04	0.78±0.04	0.72±0.04	0.04±0.04
3.4	3.7±0.2	2.7±0.1	0.16±0.04	2.9±0.1	2.5±0.1	0.07±0.04

Table 1 Polarization sensitivity in a planar Ge(Li) detector at a gamma ray energy of 0.847 MeV.

Energy (MeV)	One-Compton Events			All Events		
	ε_{mean} ω=0 (mm)	ε_{mean} ω=90 (mm)	Q	ε_{mean} ω=0 (mm)	ε_{mean} ω=90 (mm)	Q
0.400	3.3±0.2	2.2±0.1	0.20±0.05	3.4±0.2	3.1±0.2	0.05±0.05
0.847	3.7±0.2	2.7±0.1	0.16±0.04	2.9±0.2	2.5±0.1	0.07±0.04
1.500	3.2±0.2	3.0±0.2	0.03±0.06	2.3±0.1	2.4±0.1	-0.02±0.04

Table 2 Polarization sensitivity as a function of gamma ray energy in a planar detector of thickness 3.4 cm.

Multicompton Events and Pair Production Since ξ measurements are dependent only upon the two outermost events in the crystal, ξ spectra from multicompton events tend also to be polarization insensitive. Thus at larger energies (>1 MeV) where multicompton and pair production events dominate over one-compton events, the detector will again lose its polarization sensitivity.

Scattering Angle Θ The average scattering angle Θ is dependent upon the energy of the incoming gamma, in that as the energy increases, the average angle Θ decreases. This preference at higher energies towards forward scattering will further decrease any polarization sensitivity inherent in the ξ measurements.

These then are the major factors which dictate the shape of a particular ξ spectrum. Other lesser factors could be included (see fig. 13), but the arguments given above represent the main limitations to polarization measurement by this new method.

Results:

The results of various Monte-Carlo computing programs are summarized in tables 1 and 2. The computer simulated a detector of radius 1.73 cm and thickness either 0.6 cm or 3.4 cm, and again assumed that all pulse shapes were sharp. It should be noted here that any device capable of making ξ measurements most likely would not be able to distinguish one-compton events from all other inter-

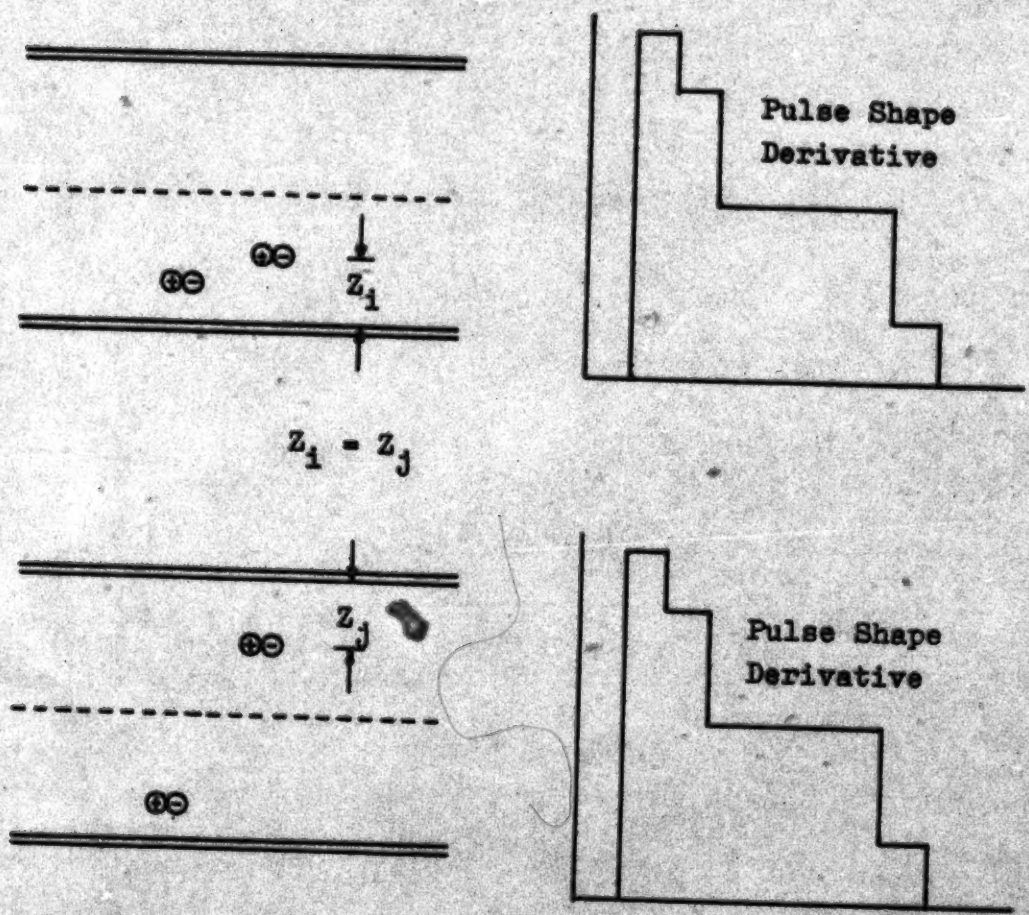

Figure 13 Identical Pulse Shape Derivatives

Note that an $\mathcal{E}$ measuring device would not be able to distinguish between these two different one-compton interactions.

actions. Therefore the right side of table 2 is in fact the best representation of what real experimental results would look like.

Chapter IV

Conclusions

It should now be possible to compare the various polarimeters mentioned above. To begin with, of the two pulse shape measurement devices discussed, the ξ measuring device appears to be the more polarization sensitive. This is logical since its output is directly related to the separation along a particular axis of the two gamma interactions in a one-compton scattering event, and it is this separation which is directly related to the polarization.

Next, a comparison can be made between the polarization sensitivity Q of the ξ device, and the sensitivities of the three other conventional polarimeters (see table 3). This table shows that, at an energy of 0.847 MeV, the ξ device has a Q value of about the same magnitude as the thin planar detector, which is of course considerably less than the sensitivities of either the two- or three-crystal polarimeters. Furthermore, whereas the ξ polarimeter suffers from the same low energy difficulties as the planar detector, (an inability to distinguish between photoelectric and one-compton events), it also suffers from a few high energy (>1 MeV) problems which the planar detector does not encounter. These include its inability to distinguish between one-compton and many-compton events, and the increasing electron range R_e which tends to smear out pulse shapes.

Type Of Polarimeter	Polarization Sensitivity
Three-Crystal)[3]	0.44±0.02
Two-Crystal)[4]	0.35±0.03
Planar Detector)[5]	0.08±0.05
ℰ Measurement Device	0.07±0.04

Table 3 Polarization sensitivity of various Ge(Li) polarimeters at a gamma ray energy of 0.847 MeV.

Further experimental study could be carried out to verify the computer results given above. However, this would require the design and construction of a new pulse shape discriminator, and the purchase of a new Ge(Li) detector which would be at least as thick as the one simulated above. In light of the comparisons just made, it is my opinion that this extra work and expense would not be meritted. If in the future it becomes necessary to make gamma-ray polarization measurements, then it is my suggestion that a conventional two- or three-crystal polarimeter be built.

References

1) White, D.C.S., The Measurement of Subnanosecond Nuclear Lifetimes, Ph.D. Thesis, University of Alberta, 1974

2) Sherman, I.S., Strauss, M.G., Nucl. Instr. and Meth. 117(1974)285

3) Butler, P.A., Carr, P.E., Gadekon, L.L., James, A.N., Nolan, P.J., Sharpey-Schafer, J.F., Twin, P.J., Viggars, D.A., Nucl. Instr. and Meth. 108(1973)497

4) Bass, R., Brinkmann, S., Von Charzewski, C., Hanle, H., Nucl. Instr. and Meth. 104(1972)33

5) Litherland, A.E., Ewan, G.T., Lam, S.T., Can. J. Phys. 48(1970)2320

Appendix 1

Polarization Effects In Photoelectric Absorption

One problem encountered when trying to develop a single crystal gamma polarimeter was that, at low energies photoelectric absorption predominates over compton scattering. It would thus be very useful if any polarization sensitivity inherent in the photoelectric effect could be used to make gamma ray polarization measurements.

Photoelectric absorption can occur when a gamma photon encounters an electron in the vicinity of an atom's nucleus. Virtually all of the energy of the photon is absorbed by the electron, although the presence of the nucleus is essential in order to conserve linear momentum, and the electron is ejected from the atom in some preferential direction. The differential cross section for the ejection of electrons from the atomic K-shell at low energies is given by:

$$\frac{d\sigma}{d\Omega} = R Z^5 \left(\frac{1}{\alpha}\right)^{7/2} \frac{\sin^2\theta \cos^2\phi}{[(1+\gamma/2)^2 - \beta\cos\theta]^4}$$

where $\beta = \frac{v}{c}$, $\alpha = \frac{E_\gamma}{m_e c^2}$,

Z is the atomic number of the absorbing material,

R is a constant, and

θ and ϕ are as previously defined in fig. 1, in which the scattered photon is now replaced by the recoiling electron.

It is obvious from this equation that at low energies

electrons will be preferentially ejected in the $\Theta = 90^\circ$ and $\phi = 0^\circ$ direction; that is in the direction of the electric vector of the incident radiation.

At relativistic energies, the differential cross section must be modified to become:

$$\frac{d\sigma}{d\Omega} \approx C(A + B\cos^2\phi)$$

where $A = (\alpha^2/4)(1-\beta\cos\Theta)$

$B = (1-\beta^2)^{\frac{1}{2}} - (\alpha/2)(1-\beta\cos\Theta)$

and $C = (1/\alpha)^4(1-\beta^2)^{\frac{1}{2}}\beta^2\sin^2\Theta/(1-\beta\cos\Theta)^4$

A simple interpretation of this equation similar to that given for the low energy case is no longer possible. However it can be stated that the angle Θ_{max} for which the differential cross section intergrated over ϕ is a maximum decreases as the energy of the incoming gamma increases. As well the asymmetry ratio $A(\Theta)$ defined by:

$$A(\Theta) = \frac{d\sigma(\phi=0^\circ) - d\sigma(\phi=90^\circ)}{d\sigma(\phi=0^\circ) + d\sigma(\phi=90^\circ)}$$

decreases for $\Theta = \Theta_{max}$ as the energy increases. These two relations are shown graphically in fig. 14.

In trying to measure this polarization asymmetry, it is of course impossible to directly detect in which direction the electrons are ejected. At best it is possible to visualize, in some way, the "track" the electron makes as it scatters and loses energy by ionization inside a detector. (For instance, when using a planar Ge(Li) detector and a pulse shape analyser

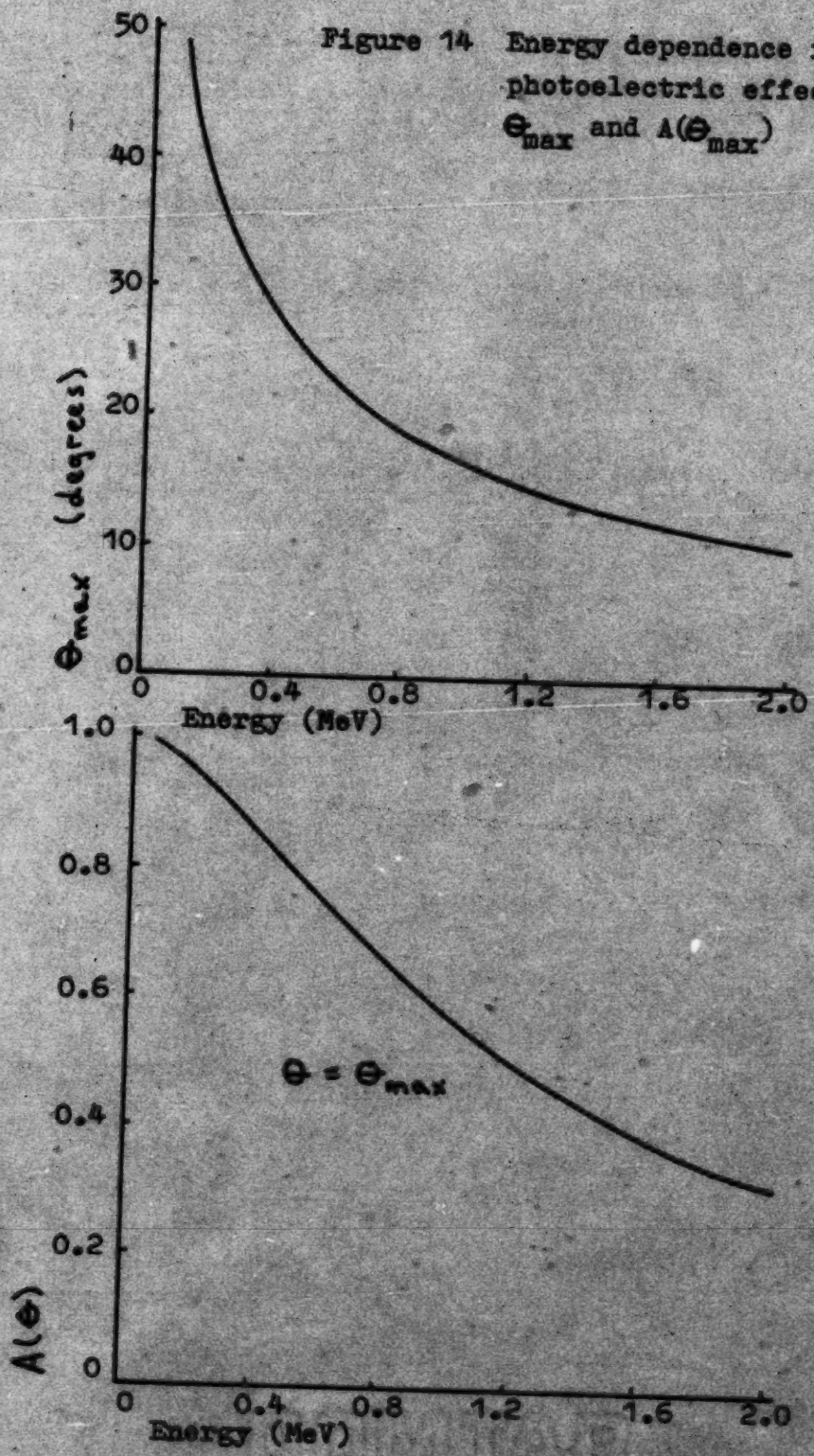

Figure 14 Energy dependence in the photoelectric effect of θ_{max} and $A(\theta_{max})$

similar to either one of the two described above, it is theoretically possible to measure the projection of an electron's ionization track on a line perpendicular to the plane of the detector.) Hence it is essential that photoelectrons not only be ejected from their atoms in some prefered direction, but also that they continue to travel in relatively straight lines as they lose energy. Otherwise the electrons will "forget" in which direction they were originally ejected, and any polarization sensitivity inherent in their ejection will be lost.

A simplified theory of electron multiple scattering can be used to estimate just how straight the electron tracks will be. This theory assumes that the electrons only undergo deflection by Rutherford scattering off atomic nuclei, and that these deflections are small. This type of scattering is described by the cross section:

$$\frac{d\sigma}{d\Omega} = 4Z^2 \frac{e^4}{(pc\beta)^2} \frac{1}{\theta^4} \quad ; \quad \theta \ll 1$$

where p is the electron's momentum. After travelling a distance d, a beam of electrons originally all moving in the same direction will have a spectrum of directions approximately gaussian in shape and with a standard deviation:

$$\langle \theta^2 \rangle = 8\pi N Z^2 e^4 \int_0^d \frac{K}{(pc\beta)^2} \, dx$$

where of course it must be kept in mind that $pc\beta$ will decrease as the distance travelled increases. N here

refers to the number of atoms in the detector per unit volume, while K is given by:

$$K = \ln(\Theta_{max}/\Theta_{min})$$

where Θ_{max} now represents the maximum scattering angle in any one collision, and Θ_{min} the minimum scattering angle. In this appendix it will be assumed that $\Theta_{max} \approx 5^\circ$ and $\Theta_{min} \approx 0.1^\circ$ so that K is a constant. This assumption will not greatly effect the final conclusions to the appendix due to the insensitivity of the logarithmic function.

At an energy of 1 MeV, about 96% of the energy loss of an electron is due to ionization. Hence the further approximation is made that:

$$\frac{dT}{dx} = \frac{dT}{dx}\Big)_{ion}$$

$$= \frac{2\pi e^4 NZ}{m_o c^2 \beta^2}\left[\ln\left(\frac{m_o c^2 \beta^2 T}{I^2(1-\beta^2)}\right) - \beta^2\right]$$

where T is the kinetic energy of the electron, and I the ionization energy of an atomic electron. If this equation is combined with the previous expression for $\langle\Theta^2\rangle$, then the change in $\langle\Theta^2\rangle$ with distance travelled can be calculated for any starting electron energy. Some examples of these results are shown graphically in fig. 15. These results can be compared with fig. 16 which plots electron kinetic energy T as a function of distance travelled. In both figures it is assumed that the electron scatters inside a germanium crystal.

One can clearly see from these graphs that the

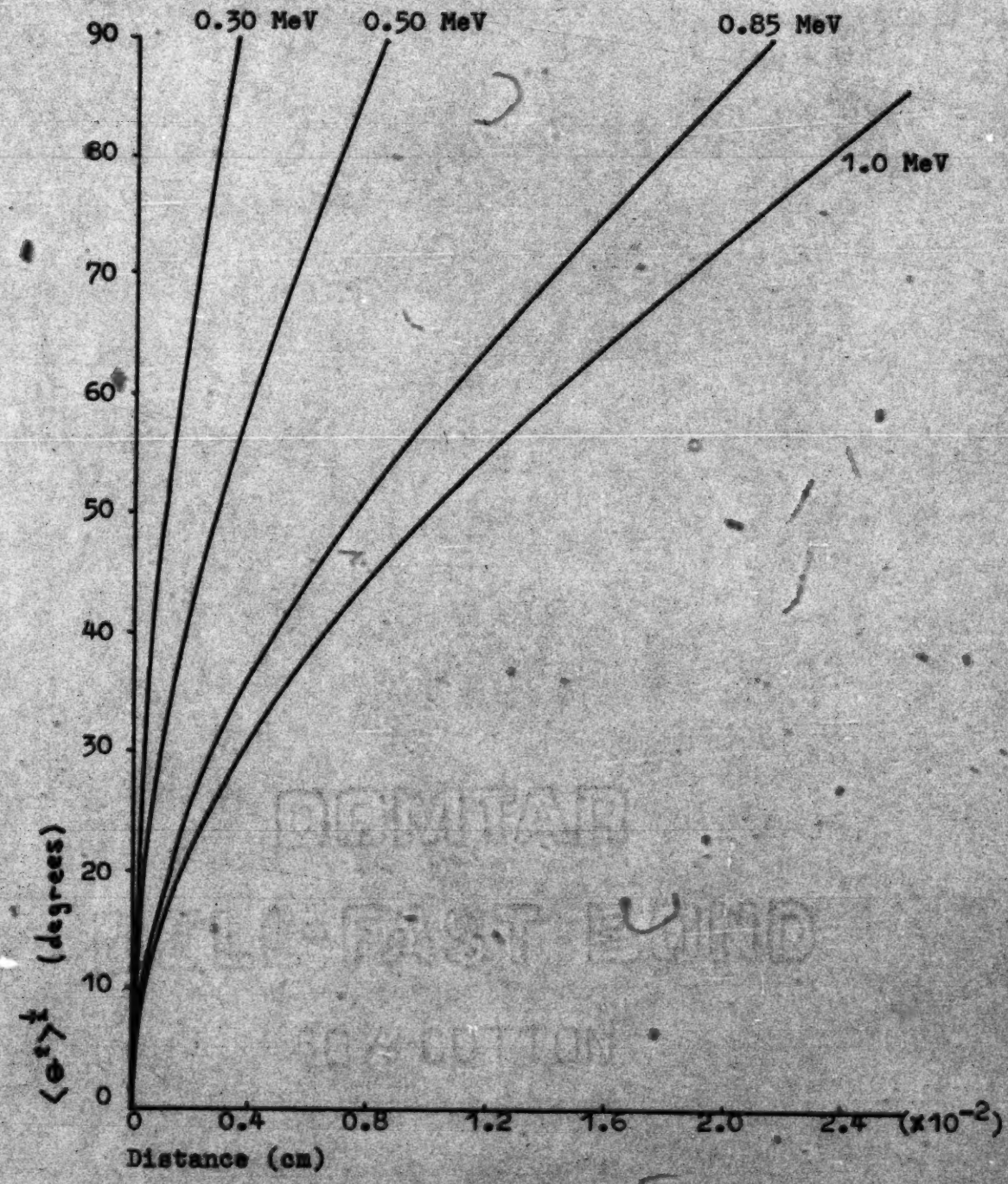

Figure 15 Average spreading of electrons as a function of distance travelled in a Ge(Li) detector.

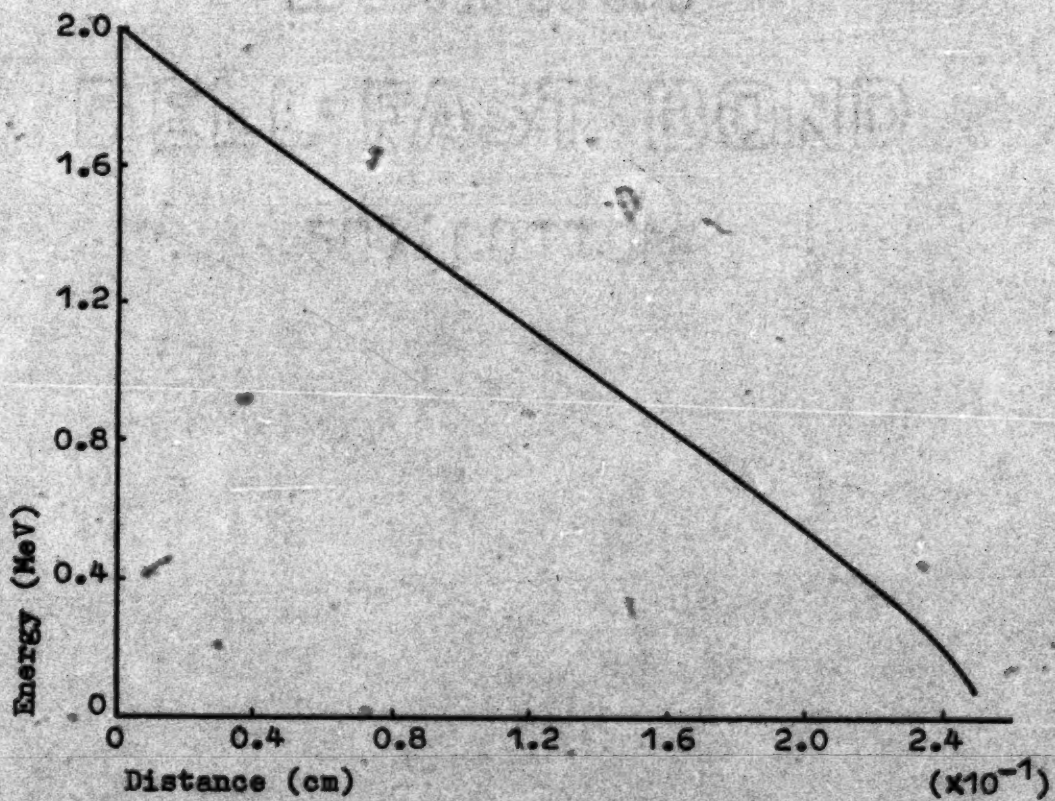

Figure 16 Electron energy as a function of total distance travelled in a Ge(Li) detector.

electrons forget in which direction they were originally ejected long before they come to a complete stop in the detector. Thus it is quite doubtful if the photoelectric effect could be used in a Ge(Li) detector as the basis of any practical polarization measurement techniques.

Appendix 2

Monte-Carlo Compton Scattering Simulation Program

A Monte-Carlo computing program was written in FORTRAN IV to simulate the scattering of gamma photons inside a planar Ge(Li) detector. The data produced by this program was then used as input to several other programs, which in turn produced the results shown in fig. 10 and tables 1 and 2. A brief explanation of this program, followed by a listing of it, is given below. All numbers in parentheses refer to line numbers in the listing.

In this simulation, a cylindrical planar detector of thickness DLE and radius RO2 is assumed. The detector dimensions, measured in centimeters, can easily be changed (see lines 10,11,337), but are not actual input variables. The program does require as input the initial gamma ray energy EN in MeV, a random number seed ISET which will be explained later, the total number of gamma photons NN which the program will simulate, and the beam polarization angle XPH1 in degrees. XPH1 corresponds to the detector orientation angle ω shown in fig. 2, where all gamma rays are considered to have a polarization of +1.

The program is structured in such a way that a gamma photon entering the planar detector edge on must have its first gamma interaction somewhere inside the detector crystal (56-81). It then determines whether

this gamma photon will be photo-absorbed or compton scattered (86,87), and if photo-absorption takes place, returns to line 52 to consider the next gamma ray entering the crystal. If compton scattering occures, however, it calculates the scattering angles θ (94-106), ϕ (109-120), and β (139-142) as defined in fig. 1, and as well the energy of the compton scattered photon (130-134). It then decides where the next gamma interaction will take place (137, 148-165), and whether or not this location is inside the detector (169, 170). If the gamma ray has been scattered outside the detector the program ignores this photon and returns to line 52 to begin again. Otherwise the program returns to line 86 to ask if the gamma ray will now be photo-absorbed or compton scattered again.

This process is continued untill the gamma ray is either scattered outside the crystal, or totally absorbed in it. If the photon is totally absorbed, the program keeps track of where each gamma interaction takes place (192), and how much energy is lost with each interaction (193).

After the specified number of incident gamma rays have been studied, the program outputs (198) the total number of photons which escaped the detector (JJ), were photo-absorbed (KK), were compton scattered only once (KL), were compton scattered twice (KM), and were compton scattered more than twice (KN). It also outputs the total number of counts in the full energy peak (200),

which is of course just the sum of KK, KL, KM, and KN.

A number of subroutines are used throughout the program. These are outlined below.

SUBROUTINE INRAND uses a random number seed ISET generated by the user to initialize a sequence of random numbers. The subroutine is thereafter entered from the main program at the statement ENTRY RAND (215), which generates a random number RA between 0 and 1.

SUBROUTINE DETR determines the range of the gamma ray in the germanium crystal.

SUBROUTINE THPR determines the probability of a compton scatter occuring at an angle Θ for any angle ϕ.

SUBROUTINE PHPR determines the probability of a compton scatter occuring at an angle ϕ for a specific angle Θ.

SUBROUTINE POPR determines the angle β associated with a particular gamma ray scattered at given angles Θ and ϕ.

SUBROUTINE COORD converts from the scattering coordinates Θ, ϕ and β to the detector coordinates.

SUBROUTINE PERC determines if a gamma photon of a particular energy will be photo-absorbed or compton scattered.

SUBROUTINE OUT determines if a particular gamma is inside or outside the detector crystal.

```
      1      C
      2      C THIS PROGRAM SIMULATES COMPTON SCATTERING AND PHOTO-ABSORPTION
      3      C INSIDE A GE(LI) DETECTOR,
      4      C
      5      C
      6            DIMENSION ER(10),CET(10),SET(10),CEP(10),SEP(10),CBE(10),SBE(10)
      7            DIMENSION Z(10),W(10)
      8            COMMON /A/X2,Y2,Z2/B/FCET,FSET,FCEP,FSEP,FCBE,FSBE
      9            COMMON /C/X1,Y1,Z1
     10            DATA PI,AN,CONST,DLE/3.14159,0.0442,0.3592,3.4/
     11            DATA RO2/1.73/
     12      C
     13      C
     14       10   FORMAT(I6)
     15       12   FORMAT(F7.4)
     16       16   FORMAT(I2)
     17       20   FORMAT(F7.0)
     18       28   FORMAT(F8.3)
     19       34   FORMAT(1X,//,'ENERGY = ',F7.4,5X,'ALPHA = ',F7.4,5X,'# OF LOOPS =
     20           *',I8)
     21       36   FORMAT(1X,/,'# ESCAPING DETECTOR = ',I8,2X,'# ABSORBED = ',I8,' PH
     22           *OTO',2X,I8,' =1 COMP',2X,I8,' =2 COMP',2X,I8,' >2 COMP')
     23       38   FORMAT(1X,3(3X,F7.4))
     24      C
     25      C
     26      C INPUT ENERGY, RANDOM NUMBER SEED AND NUMBER OF LOOPS
     27      C
     28        1  READ(5,12)EN
     29           IF(EN.EQ.0.)GO TO 130
     30           ALT=EN/.511
     31           SIGPE1=CONST/(ALT**3.5)
     32           CALL THPR(ALT,PI,TOTCR1)
     33           RMIN=(-RO2)*2.*AN*(TOTCR1+SIGPE1)
     34           RMIN=EXP(RMIN)
     35           READ(5,16)ISET
```

```
:      36              CALL INRAND(ISET)
:      37              READ(5,20)ZZ
:      38              NN=INT(ZZ)
:      39        C
:      40        C  INPUT BEAM POLARIZATION ANGLE
:      41        C
:      42              READ(5,28)XPH1
:      43              XPH1=XPH1*PI/180.
:      44        C
:      45        C
:      46         40   LL=0
:      47              JJ=0
:      48              KK=0
:      49              KL=0
:      50              KM=0
:      51              KN=0
:      52         55   PH1=XPH1
:      53        C
:      54        C DETERMINE INITIAL GAMMA POSITION IN DETECTOR
:      55        C
:      56         60   CALL RAND(RA)
:      57              Y0=(.5-RA)*2.*RO2
:      58              CALL RAND(RA)
:      59              Z0=(.5-RA)*DLE
:      60              TOTCR=TOTCR1
:      61              SIGPE=SIGPE1
:      62              AL=ALT
:      63              CALL RAND(PA)
:      64              RA=(RA*(1.-RMIN))+RMIN
:      65              B=ALOG(RA)
:      66              EX=(-B)/(AN*(TOTCR+SIGPE))
:      67              XPLUS=(RO2*RO2)-(Y0*Y0)
:      68              XPLUS=RO2-SORT(XPLUS)
:      69              EX=EX*(RO2-XPLUS)/RO2
:      70              X0=XPLUS+EX
```

```
      71              SQ=(X0*X0)+(Y0*Y0)+(RO2*RO2)-(2.*X0*RO2)
      72              DR=SQRT(SQ)
      73              IF(DR.GT.RO2) GO TO 55
      74              NUM=0
      75              CTHI=COS(PH1)
      76              STHI=SIN(PH1)
      77              DO 63 JV=1,10
      78              Z(JV)=0.
      79        63    W(JV)=0.
      80              JV=1
      81              Z(JV)=2.*ABS(Z0)/DLE
      82        C
      83        C
      84        C
      85        C
      86         65   CALL PERC(AL,TOTCR,SIGPE,ISIG)
      87              IF(ISIG.EQ.0)GO TO 90
      88        C
      89        C COMPTON SCATTERING OF GAMMA BEGINS
      90        C
      91              NUM=NUM+1
      92              IF(NUM.GT.10) GO TO 85
      93        C
      94              STEP=PI/2.
      95              XX1=STEP
      96              CALL RAND(RA)
      97              DO 70 I=1,7
      98              STEP=STEP/2.
      99              CALL THPP(AL,XX1,YY1)
     100              YY1=YY1/TOTCR
     101              IF(YY1.GT.RA)GO TO 68
     102              XX1=XX1+STEP
     103              GO TO 70
     104        68    XX1=XX1-STEP
     105        70    CONTINUE
```

```
:     106        72   ET=XX1
:     107      C
:     108      C
:     109           STEP=PI
:     110           XX1=STEP
:     111           CALL RAND(RA)
:     112           DO 80 I=1,8
:     113           STEP=STEP/2.
:     114           CALL PHPR(AL,ET,XX1,YY1)
:     115           IF(YY1.GT.RA)GO TO 75
:     116           XX1=XX1+STEP
:     117           GO TO 80
:     118        75 XX1=XX1-STEP
:     119        80 CONTINUE
:     120        81 EP=XX1
:     121      C
:     122      C
:     123           CET(NUM)=COS(ET)
:     124           SET(NUM)=SIN(ET)
:     125           CEP(NUM)=COS(EP)
:     126           SEP(NUM)=SIN(EP)
:     127      C
:     128      C DETERMINE NEW GAMMA ENERGY AFTER COMPTON SCATTER
:     129      C
:     130           AL1=AL
:     131           AL=1.-CET(NUM)*(1./AL)
:     132           AL=1./AL
:     133           AL2=AL
:     134           W(JV)=(AL1-AL2)/ALT
:     135           SIGPE=CONST/(AL**3.5)
:     136           CALL THPR(AL,PI,TOTCP)
:     137           CALL DETR(TOTCR,SIGPE,ER(NUM))
:     138      C
:     139           X2=0.
:     140           Y2=0.
```

```
      141          Z2=0.
      142          CALL POPR(CET(NUM),SET(NUM),CEP(NUM),AL,PI,BE)
      143          CBE(NUM)=COS(BE)
      144          SBE(NUM)=SIN(BE)
      145    C
      146    C DETERMINE NEW LOCATION OF GAMMA IN DETECTOR
      147    C
      148     83   DO 84 I=1,NUM
      149          J=NUM-I+1
      150          X2=X2+ER(J)
      151          FCET=CET(J)
      152          FSET=SET(J)
      153          FCEP=CEP(J)
      154          FSEP=SEP(J)
      155          FCBE=CBE(J)
      156          FSBE=SBE(J)
      157          CALL COORD
      158     84   CONTINUE
      159    C
      160          Y3=(Y2*CTHI)-(Z2*STHI)
      161          Z2=(Y2*STHI)+(Z2*CTHI)
      162          Y2=Y3
      163          X1=X0+X2
      164          Y1=Y0+Y2
      165          Z1=Z0+Z2
      166    C
      167    C IS GAMMA STILL IN DETECTOR?
      168    C
      169          CALL OUT(IOUT,DZ)
      170          IF(IOUT.EQ.0)GO TO 85
      171          JV=JV+1
      172          Z(JV)=2.*DZ/DLE
      173          GO TO 65
      174    C
      175     85   JJ=JJ+1
```

```
:     176              GO TO 110
:     177        C
:     178        C OUTPUT
:     179        C
:     180         90   IF(NUM.EQ.0) GO TO 92
:     181              IF(NUM.EQ.1) GO TO 95
:     182              IF(NUM.EQ.2) GO TO 97
:     183              GO TO 100
:     184         92   KK=KK+1
:     185              GO TO 105
:     186         95   KL=KL+1
:     187              GO TO 105
:     188         97   KM=KM+1
:     189              GO TO 105
:     190        100   KN=KN+1
:     191        105   W(JV)=AL/ALT
:     192              WRITE(7,38) (Z(I),I=1,10)
:     193              WRITE(8,38) (W(I),I=1,10)
:     194        110   LL=LL+1
:     195              IF(LL.GE.NN)GO TO 120
:     196              GO TO 55
:     197        120   WRITE(6,34)EN,ALT,NN
:     198              WRITE(6,36)JJ,KK,KL,KM,KN
:     199              KT=NN-JJ
:     200              WRITE(9,10) KT
:     201              GO TO 1
:     202        130   STOP
:     203              END
:     204        C
:     205        C
:     206              SUBROUTINE INRAND(ISET)
:     207              DIMENSION ISTART(5)
:     208              DATA ISTART/718415745,1039450965,998356979,124005191,1035693051/
:     209              DATA MULT/32771/
:     210              DATA ISIZE /1073741824/
```

FOR OFFICIAL USE ONLY

```
:     211              DATA RNORM /2147483648./
:     212              KSET=MOD(ISET,5)
:     213              IRAND=ISTART(KSET+1)
:     214              RETURN
:     215              ENTRY RAND(RA)
:     216              IRAND=MOD(IRAND*MULT,ISIZE)
:     217              RA=FLOAT(IRAND)/RNORM
:     218              RA=RA+.5
:     219              RETURN
:     220              END
:     221        C
:     222        C
:     223              SUBROUTINE DETR(TOTCR,SIGPE,ER)
:     224              DATA AN/0.0442/
:     225              CALL RAND(RA)
:     226              B=ALOG(RA)
:     227              ER=(-B)/(AN*(TOTCR+SIGPE))
:     228              RETURN
:     229              END
:     230        C
:     231        C
:     232              SUBROUTINE THPR(AL,ET,PRT)
:     233              XC=COS(ET)
:     234              B=1.+(AL*(1.-XC))
:     235              XL=ALOG(B)
:     236              B=1./B
:     237              XA1=1./AL
:     238              XA2=XA1*XA1
:     239              XA3=XA2*XA1
:     240              APO=AL+1.
:     241              C=(XA1*XL)-(XA1/2.)-(B*B*XA1/2.)
:     242              D=(B*XA1)+(APO*APO*XA3)+((1.-XC)*XA2)
:     243              E=(2.*APO*XL*XA3)+(APO*APO*B*XA3)
:     244              PRT=C+D-E
:     245              PRT=8.*PRT
```

```
      246            RETURN
      247            END
      248      C
      249      C
      250            SUBROUTINE PHPR(AL,ET,EP,PRP)
      251            THCS=COS(ET)
      252            THSQ=1.-(THCS*THCS)
      253            PH2=2.*EP
      254            PHSN=SIN(PH2)
      255            C=1.+(AL*(1.-THCS))
      256            B=1./C
      257            D=EP/(2.*3.14159)
      258            E=(THSQ*PHSN)/(4.*3.14159*(C+B-THSQ))
      259            PRP=D-E
      260            RETURN
      261            END
      262      C
      263      C
      264            SUBROUTINE POPR(CET,SET,CEP,AL,PI,XX1)
      265            CALL RAND(RA)
      266            V=1.+(AL*(1.-CET))
      267            V=V+(1./V)
      268            CSQ2=SET*SET*CEP*CEP
      269            SSQ2=1.-CSQ2
      270            C=2.*PI*(V-(2.*CSQ2))
      271            STEP=PI
      272            XX1=STEP
      273            DO 15 I=1,8
      274            STEP=STEP/2.
      275            XX2=2.*XX1
      276            A=XX1+(SIN(XX2)/2.)
      277            B=2.*SSQ2*A
      278            YY1=(XX1*(V-2.))+B
      279            YY1=YY1/C
      280            IF(YY1.GT.RA) GO TO 10
```

```
:     281              XX1=XX1+STEP
:     282              GO TO 15
:     283        10    XX1=XX1-STEP
:     284        15    CONTINUE
:     285              RETURN
:     286              END
:     287        C
:     288        C
:     289              SUBROUTINE COORD
:     290              COMMON /A/X2,Y2,Z2/B/CET,SET,CEP,SEP CBE,SBE
:     291              DIMENSION A(3,3),X(2,3)
:     292              CSQ=SET*CEP
:     293              SSQ2=1.-(CSQ*CSQ)
:     294              SSQ=SQRT(SSQ2)
:     295              CPH=1.+CET-SSQ
:     296              SPH2=1.-(CPH*CPH)
:     297              SPH=SQRT(SPH2)
:     298        C
:     299              A(1,1)=SSQ*CPH
:     300              A(1,2)=-(CSQ*CPH*CBE)+(SBE*SPH)
:     301              A(1,3)=(CSQ*CPH*SBE)+(CBE*SPH)
:     302              A(2,1)=CSQ
:     303              A(2,2)=CBE*SSQ
:     304              A(2,3)=-(SBE*SSQ)
:     305              A(3,1)=-(SSQ*SPH)
:     306              A(3,2)=(CSQ*SPH*CBE)+(SBE*CPH)
:     307              A(3,3)=-(CSQ*SPH*SBE)+(CBE*CPH)
:     308        C
:     309              X(1,1)=X2
:     310              X(1,2)=Y2
:     311              X(1,3)=Z2
:     312        C
:     313              DO 20 J=1,3
:     314              X(2,J)=0.
:     315              DO 20 K=1,3
```

```
:     316          20   X(2,J)=X(2,J)+(A(J,K)*X(1,K))
:     317               X2=X(2,1)
:     318               Y2=X(2,2)
:     319               Z2=X(2,3)
:     320               RETURN
:     321               END
:     322          C
:     323          C
:     324               SUBROUTINE PERC(AL,TOTCR,SIGPE,ISIG)
:     325               PERC=TOTCR/(TOTCR+SIGPE)
:     326               CALL RAND(RA)
:     327               IF(RA.GT.PERC)GO TO 10
:     328               ISIG=1
:     329               RETURN
:     330          10   ISIG=0
:     331               RETURN
:     332               END
:     333          C
:     334          C
:     335               SUBROUTINE OUT(IOUT,DZ)
:     336               COMMON /C/X1,Y1,Z1
:     337               DATA RO2,DLE/1.73,3.4/
:     338               SQ=(X1*X1)+(Y1*Y1)+(RO2*RO2)-(2.*X1*RO2)
:     339               DR=SQRT(SQ)
:     340               IF(DR.GT.RO2)GO TO 10
:     341               DZ=ABS(Z1)
:     342               Z=DLE/2.
:     343               IF(DZ.GT.Z)GO TO 10
:     344               IOUT=1
:     345               RETURN
:     346          10   IOUT=0
:     347               RETURN
:     348               END
:
```